Strojnícky časopis – *Journal of* MECHANICAL ENGINEERING,
VOL 72 (2022), NO 1, 15 – 22

COMPARISON OF FEM SIMULATIONS OF RUBBER-METAL MOUNT ELEMENT

BUCHA Jozef[1], DANKO Ján[1*], MILESICH Tomáš[1], NEMEC Tomáš[1], MAGDOLEN Ľuboš[1]

[1] *Faculty of Mechanical Engineering, Slovak University of Technology in Bratislava,Institute of Transport Technology and Engineering Design, Nám. Slobody 17,812 31 Bratislava, Slovakia,*
e – mail: jan.danko@stuba.sk

Abstract: Increasing of electric vehicles volume brings new challenges in NVH (noise, vibration and harshness) area. Presented paper deals with comparison of simulations of rubber-metal motor mount using finite element method. For the future work it is important to define static characteristics of rubber-metal mounts. It leads to study possibilities of simulations of rubber-metal mount in different software environment. Preparing of computational models are realized in MSC Marc and MSC Nastran. Results from simulations are compared to Abaqus simulation results.

KEYWORDS: FEM, Rubber-metal engine mount component, Mooney-Rivlin Elastomer Model, Static stiffness

1 Introduction

With the transition to electric mobility, the demands on NVH's (noise vibration and harshness) behavior are increasing. The development of battery electric vehicles has come to the fore, mainly due to legislation and clean mobility trends. Although the complexity of electric drives is lower than the complexity of drives powered by conventional internal combustion engines, the demands placed on NVH are in fact increasing [1]. There are two main factors:

- lower noise level due to the lack of masking effect created by the internal combustion engine
- the current level of expertise in the development of noise, vibration and hardness for electric vehicles is not yet as well established as in the case of conventional cars [1]

The setting of NVH objectives and the ongoing evaluation of these objectives during the development process are based on various subjective and objective criteria. In conventional vehicles, engine noise is the dominant element of interior noise, especially at lower speeds. Rolling noise and wind noise begin to show with the increased speed. In contrast, electric vehicle noise consists mostly of rolling noise and wind noise. Thus, due to the lack of an internal combustion engine, the high-frequency components of the electric drive unit are more noticeable (Fig. 1) [2].

DOI: 10.2478/scjme-2022-0002, Print ISSN 0039-2472, On-line ISSN 2450-5471

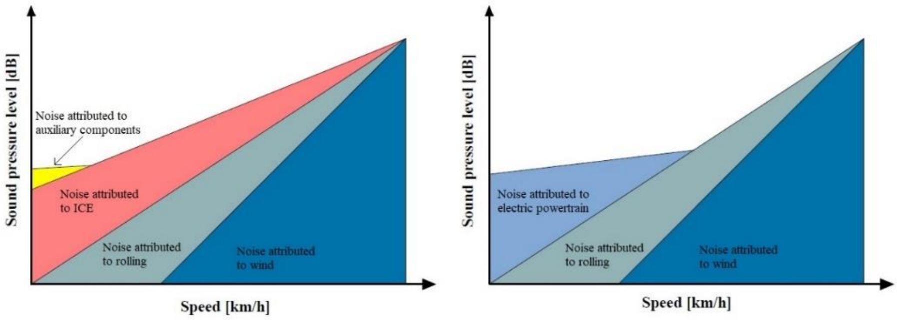

Fig. 1 Noise distribution in electric drive

The electric propulsion system usually does not emit any broadband sound levels. Nevertheless, electric cars with the lowest level of internal noise can have an unpleasant acoustic character at certain speeds and loads due to the vibrations of the drive train transmitted to the interior [3]. The system for holding electric motors and drive components should also withstand high torques and rapid torque changes during acceleration and recuperation (Fig. 2). Generally, it would be advantageous if the engine mounts preferred to remain at their original level of stiffness even at torque. It is also necessary to consider a good acoustic and vibration insulation of the high-frequency excitation [6,7] of the electric motor, which must then be ensured by the correct arrangement of the system and especially by innovations at the level of component design solutions. The easiest way to achieve load-independent behavior is to use solid rubber iron mounts. The correct choice of material and construction of the rubber metal engine mount will ensure the necessary initial rigidity and durability.

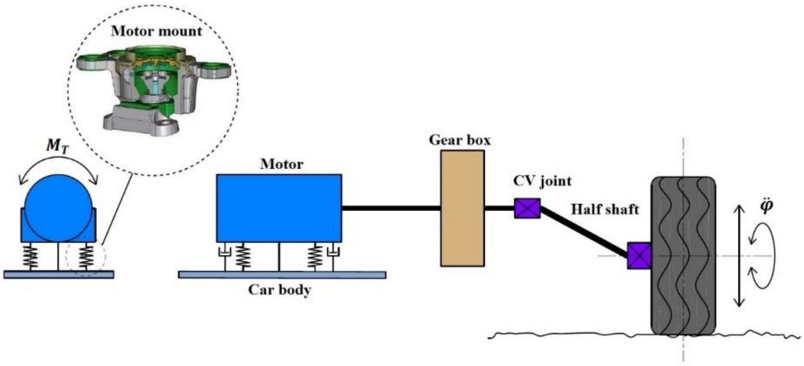

Fig. 2 Block representation of EV driveline

Therefore, the automotive industry is currently developing appropriate processes for setting targets and acceptance criteria in the field of NVH in the electrified powertrain [8]. One part of this issue is the creation of mathematical simulation processes to reduce costs and time [9].

2 Description of FEM model used in computation

Preprocessing was done using combination of MSC Apex and MSC Patran. MSC Apex was used for geometry simplification and meshing. For meshing 2.5D lofted mesher was used. Fig. 3a) shows CAD model before simplification, Fig. 1b) shows resulted 2.5D lofted linear hex mesh with size of element 1mm created in MSC Apex. In Nastran Sol400 used element type is CHEXA with 8 grid points, in Marc element class 17.

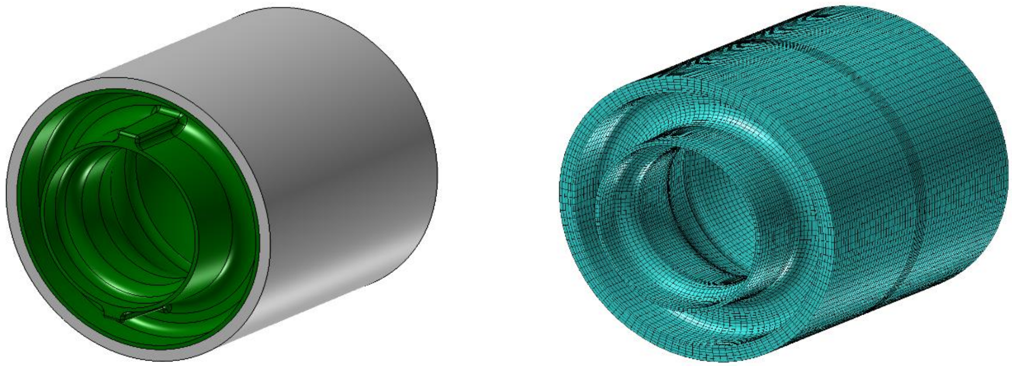

a) b)

Fig. 3 CAD model and FEM mesh of rubber metal engine mount

Rubber-metal engine mount consists of two parts (outer steel ring and inner rubber part). Material properties used in FEM model are depicted in Tab. 1. Element cells of materials are shown in Fig. 4.

Tab. 1 Material properties used in FEM model

Material	**Constitutive Model**	**Material Parameters**		
Steel	Linear Elastic	Young Modulus [MPa]	Poisson's Ratio [-]	Density [Tonne/mm^3]
		210000	0.3	7.8E-09
Rubber 55 ShA	Hyperelastic	Thermal Expansion coefficient [°C^{-1}]		Density [Tonne/mm^3]
		0.0001538		1.2E-09
		C_{10} [MPa]	C_{20} [MPa]	D_1 [MPa]
		0.484021	0.0242011	2420.1

Hyperelastic formulation used in the FEM model is based on the generalized Mooney-Rivlin polynomial function of strain energy W:

$$W = \sum_{i,j=0}^{N} C_{ij} (I_1 - 3)^i (I_2 - 3)^j + \sum_{i=0}^{N} D_i (I_3 - 1)^{2i}, \tag{1}$$

where C_{ij} are coefficients related to shear behaviour of the material, D_i describes compressibility behaviour of the material, N is order of polynomial, I_1, I_2, I_3 are strain invariants in generalized Mooney-Rivlin are defined as functions of stretch ratios $\lambda_1, \lambda_2, \lambda_3$:

$$I_1 = \lambda_1^2 + \lambda_2^2 + \lambda_3^2, I_2 = \lambda_1^2\lambda_2^2 + \lambda_2^2\lambda_3^2 + \lambda_3^2\lambda_1^2, I_{22} = \lambda_1^2\lambda_2^2\lambda_3^2. \tag{2}$$

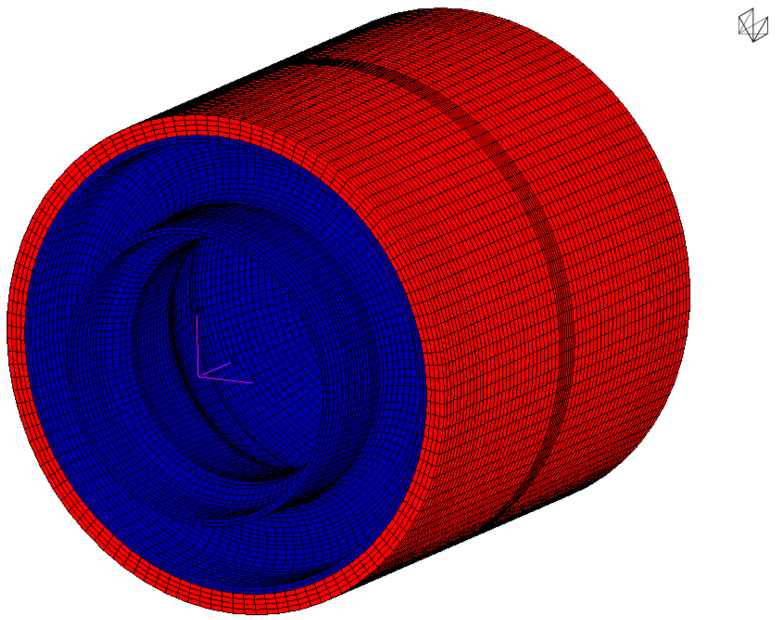

Fig. 4 Element cells used for material and element properties definition

Element properties used in FEM model were Reduced Integration, Hourglass Control (Assumed Strain) and additional integration point.

In Nastran Sol400 this is defined with auxiliary property PSLDN1 in Bulk Data Section using integration code LRIH (Linear Reduced Integration Hourglass control)

In Marc element type 117 was chosen.

Element cells of properties are the same as of materials and shown in Fig. 4.

FEM model contains one RBE2 connection with all 6 DOFs prescribed. Independent node Fig. 5b) is defined in middle of rubber – metal engine mount, as dependent nodes Fig. 5a) all inner nodes of rubber component were used.

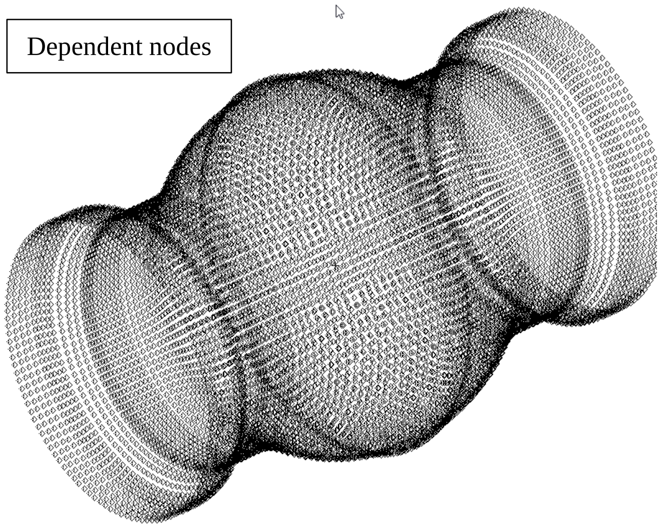

a)

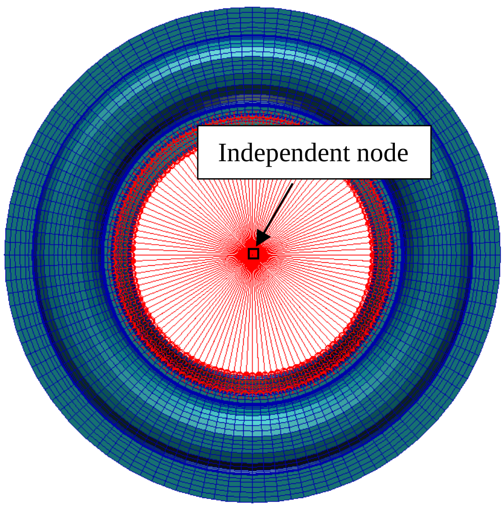

b)

Fig. 5 RBE2 connection used in model

FEM job contains three consecutive loadcases:

1. Cooldown load case: In this load case temperature is lowered from initial temperature 150 °C to 20 °C while independent node (Fig. 5b) is fixed in all 6 DOF, all outer ring surface nodes are fixed.
2. Calibration load case: In this load case temperature is maintained at 20 °C, independent node is fixed in all 6 DOF, outer ring surface nodes are displaced in radial direction (1.5 mm) using cylindrical coordinate system. Self-contact is turned on.
3. Displacement load case: In this load case temperature is maintained at 20 °C, outer ring surface nodes are fixed, independent node is displaced in desired direction using cartesian coordinate system (1 mm in x or y direction, 2 mm in z direction). Self-contact is turned on.

3 Results of FEM calculations

Fig. 6 shows the deformation of rubber metal components at the end of the third load case. Independent node was radially displaced in x-direction. Fig 6a shows front view, Fig 6b shows top view with clipping plane through middle of rubber metal component. Both figures are results of Nastran Sol400.

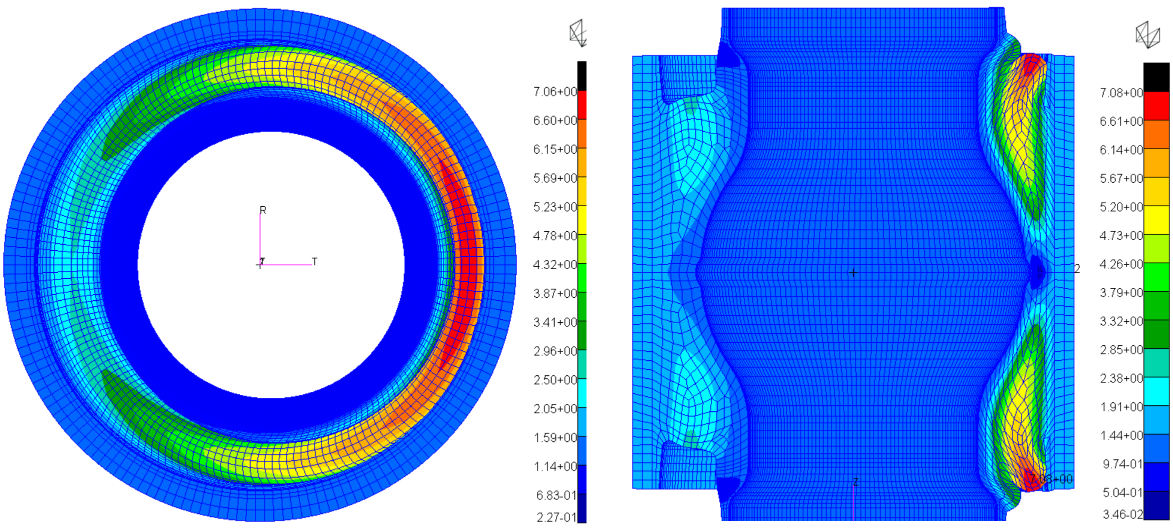

a) b)

Fig. 6 Deformation of rubber metal component – displacement in x direction

Fig. 7 shows course of computed reaction on displacement in radial direction (Third load case)

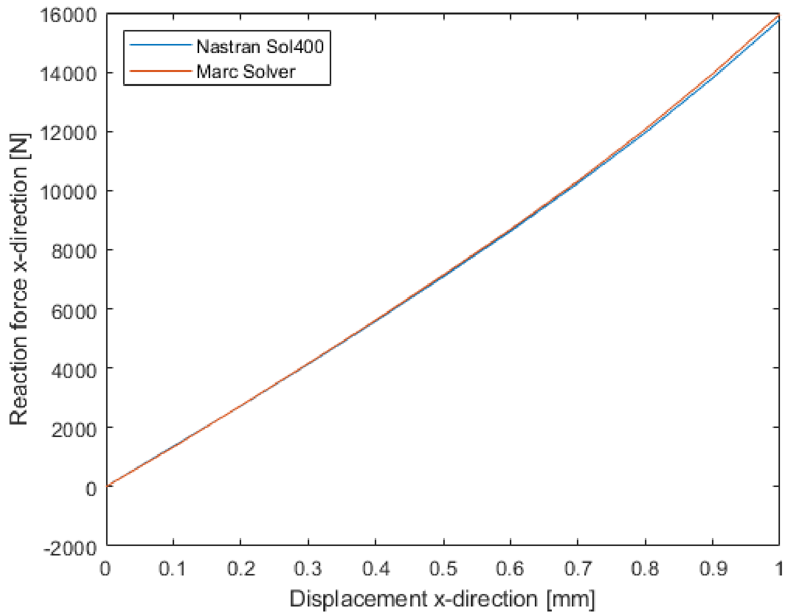

Fig. 7 Computed dependence of Reaction force on Displacement in x-direction

Fig. 8 shows the deformation of rubber metal components at the end of the third load case. Independent node was axially displaced in z-direction. Fig 8a shows front view, Fig 8b shows top view with clipping plane through middle of rubber metal component. Both figures are results of Nastran Sol400.

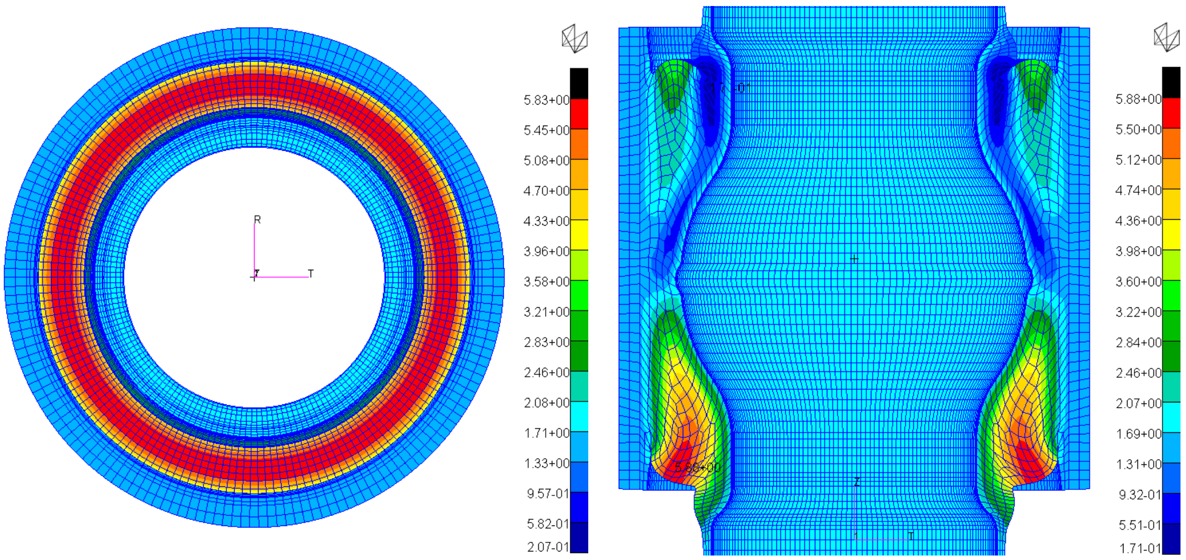

a) b)

Fig. 8 Deformation of rubber metal component – displacement in z direction

Fig. 9 shows course of computed reaction on displacement in axial direction (Third load case)

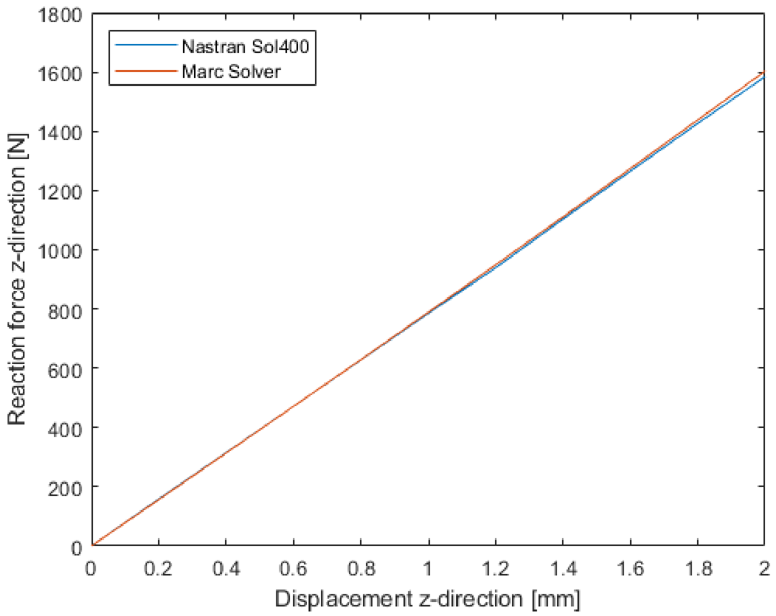

Fig. 9 Computed dependence of Reaction force on Displacement in z-direction

Tab. 2 shows values of computed axial and radial stiffness of rubber metal component and comparison with values computed from Abaqus simulation.

Tab. 2 Computed stiffness of rubber metal component

Radial stiffness		
Nastran Sol400	Marc Solver	Abaqus
14144.62 N/mm	14274.51 N/mm	13249.09 N/mm
Radial stiffness difference – Comparison to Abaqus results		
6.76 %	7.74 %	
Axial stiffness		
Nastran Sol400	Marc Solver	Abaqus
784.63 N/mm	788.32 N/mm	710.27 N/mm
Axial stiffness difference – Comparison to Abaqus results		
10.47 %	10.99 %	

CONCLUSION

Results from FEM calculations using Nastran Sol400 or Marc Solver show very good coincidence. Difference of computed stiffness between Nastran or Marc and stiffness computed from Abaqus results is caused by different mesh size and used type of solver. Both Nastran

Sol400 and Marc Solver were implicit solvers, while solver used for computation in Abaqus was explicit solver.

FEM simulation can be strong tool to evaluate and predict properties of rubber steel engine mounts. FEM models used in this paper will be compared with laboratory measured characteristics of rubber metal engine mounts and tuned to those values as needed.

Powertrains of electric vehicle are emitting vibrations in much broader frequency range than classical combustion vehicles, this produces demands not just in design of rubber metal engine mount components but also in FEM models where frequency response and properties must be in coincidence with measured data.

ACKNOWLEDGEMENT

This work was supported by the Slovak Research and Development Agency under Contract No. APVV-20-0428.

REFERENCES

[1] Ulz, A., Graf, B., Priestner, CH., Mehrgou, M. “Criteria for the NVH Development of Electric Drive Units”, ATZ Worldwide 123 (7 - 8), **2021**. DOI: 10.1007/s38311-021-0684-8

[2] Albers, A., Fisher, J., Behrendt, M., et al. “Measurement and Interpretation of the Transfer Path of an Acoustic Phenomenon in the Drivetrain of an Electric Vehicle”, ATZ Worldwide 116, **2014**. DOI: 10.1007/s38311-014-0154-7

[3] Marbjerg, G. “Noise from Electric Vehicle – Literature Survey Nr. 535”, Vejdirektoratet, **2014**. ISBN 978-87-93184-60-2

[4] “MSC Software Corporation”, MSC Nastran - Online Help [online] Available at: https://help.mscsoftware.com/ [Accessed: date (25 3 2022)].

[5] “MSC Software Corporation”, MSC Marc - Online Help [online] Available at: https://help.mscsoftware.com/ [Accessed: date (25 3 2022)].

[6] Popardovský, V. “Optimization of Vehicle Suspension Neural Model”, Proc. of the 22nd International Scientific Conference TRANSPORT MEANS 2018, Trakai, Lithuania, pp. 1361 – 1364, **2018**. ISSN 1822-296X

[7] Popardovský, V., Popardovská, E. “Vehicle Suspension Control Based on PID Controller Adapted by Feed-Forward Neural Network”, In: Zeszyty Naukowe INSTITUTU POJAZDÓW, Warsaw University of Technology, pp. 99 – 107, **2017**. ISSN 1642-347X

[8] Danko, J., Bucha, J., Milesich, T., Magdolen, L., Kevický, I., Minárik, M., Mišković, Z., Mitrović, R. “Dynamic Properties Modeling Analysis of the Rubber-Metal Elements for Electric Drive”, Strojnícky časopis – Journal of Mechanical Engineering 71 (1), pp.19 – 26, **2021**. DOI: 10.2478/scjme-2021-0002

[9] Magdolen, L., Danko, J., Milesich, T., Nemec T., Sloboda, K., Bucha, J. “Dual Mass Flywheel Parameter Identification”, Strojnícky časopis – Journal of Mechanical Engineering 71 (2), pp.167 – 178, **2021**. DOI: 10.2478/scjme-2021-0027